

## **A short study on the fabrication of single track deposits in SLM and characterization**

J.J.S. Dilip<sup>1</sup>, Md Ashabul Anam<sup>1</sup>, Deepankar Pal<sup>2,3</sup> & Brent Stucker<sup>3</sup>

<sup>1</sup>Rapid Prototyping Center, Department of Industrial Engineering, University of Louisville, Louisville, Kentucky, USA 20292.

<sup>2</sup>Department of Mechanical Engineering, University of Louisville, Louisville, Kentucky, USA 20292.

<sup>3</sup>3D SIM, 1794 Olympic Parkway, Suite 110, Park City, Utah, USA 84098.

### **Abstract**

The present investigation is focused on fabrication of single track deposits, with multiple laser power and scan speed combinations to turn understanding their effect on the formation of the melt pool. In this study alloy, IN625 powder from EOS was used to produce single track deposits. Surface morphology and dimensions of single track deposits were characterized using SEM. The cross-section of the single track deposits was studied, and the geometrical features of melt pools were evaluated. The results indicate that melt pool characteristics provide significant information that is helpful for process parameters selection. These single track experiments will be being extended to fabricate samples with multiple layers in the future study. This approach of investigating single track deposits, when used to narrow down the window of process parameters can provide a path to speed up the tedious and time-consuming experiments for optimization of process parameters.

**Keywords:** Additive manufacturing; Selective Laser Melting; Alloy IN625; Single track deposits

### **Introduction**

Additive manufacturing is categorized into a group of manufacturing technologies in which the parts are fabricated in a layer-by-layer fashion, usually from a CAD model [1]. With the excellent capabilities of additive manufacturing offers to the design capabilities, its applications span into energy, medical, aerospace, automotive and defense sectors [1,2]. Additive manufacturing processes are classified into powder bed process, powder feed processes, and wire feed processes are depending upon how the material is delivered for fusion deposition [1]. There are some commercially available additive manufacturing processes such as laser engineered net shaping, selective laser melting, electron beam melting, Ultrasonic additive manufacturing, Binder jet printing and Friction Freeform fabrication which can produce complex-shaped end-use metallic parts [1,2,3,4]. Selective Laser Melting (SLM), is a powder-bed additive manufacturing process in which successive layers of metal powder particles are melted and solidified on top of each other by a high-intensity laser beam. Some of the processes involve melting and solidification of a small volume of material deposition in the form of track-by-track and layer-by-layer. Apparently, the laser beam raster's in a line, and it melts the powder and solidifies a thin track or single track of material. A typical single track deposit is repeated with a well-defined overlap to construct a part fully [1,2,5]. Therefore, studying the single track deposits will not only provide a deeper understanding of the SLM process but also contribute to

finding a process window for processing new alloys. Fig. 1 shows a simple schematic of the track-by-track and layer-by-layer deposition that occurs during SLM process.

Recently, the number of alloys being processed using SLM are on a constant rise. Therefore optimization of process parameters is critical for achieving fully dense parts. Optimization of parameters for a new alloy is not only time consuming but also a tedious task. Therefore, in the present investigation is focused on producing of single track deposits in alloy IN625 with varying the laser power and scans speed and study the effect of parameters on the melt pool morphology. The single track information can be utilized for reducing the number of experiments for fixing optimum process parameters. Fabrication of single track deposits in SLM is not straight forward, and in order to realize single tracks, one has use carefully planned strategy in the SLM machine. Earlier studies reported on single track deposits were made on the base plate made of different alloy [6]. This study uses a base pad and advantage of using such design will have dilution effects, thus contribute to a change in the melting temperature of the alloy powder under investigation. A novel approach to fabricate single track on a base pad was employed in this work.

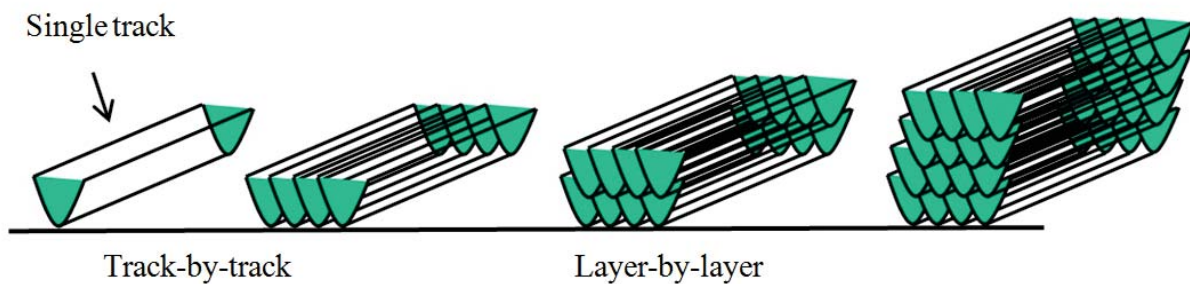


Fig.1 Schematic illustrating track-by-track and layer-by-layer deposition of material in SLM.

## Experimental work

Alloy IN625 pre-alloyed powder supplied by EOS was used in the present study. The powder was characterized using SEM for examining the particle size, shape and distribution. In order to estimate the melting temperatures of the powder differential scanning calorimetry was carried out under an inert atmosphere and using Q600 SDT, TA instruments. The heating rate was 20 C/min used. EOS M270 Direct Metal Laser Sintering (DMLS) system with Yb-fiber laser (nominal maximum power 200W) was used to fabricate the samples. Single track deposits were made using support structure strategy. A factorial design of experiment (DOE) was performed with multiple combinations of laser power and scan speeds were used to produce the single track deposits. Single track and cube samples were built using different process parameter sets as listed in Table. 1. Therefore, total 42 single track beads were designed to be made on these pads. The single line scans were placed at 5 mm apart from each other. Each pad contains six single line scan deposits with one power level. Single line scans were conducted to form single track deposits on a substrate pad of the same alloy. The base pads were built using the set of optimum parameters which yield fully dense parts. The single line scans will be made through and on the base pad. A layer thickness of 20 $\mu$ m was maintained in the experiments.

Table. 1 DOE for Single Beads with varied power and speeds.

Laser Power (W)	Scan speed (mm/s)					
50	200	400	600	800	1000	1200
75	200	400	600	800	1000	1200
100	200	400	600	800	1000	1200
125	200	400	600	800	1000	1200
150	200	400	600	800	1000	1200
175	200	400	600	800	1000	1200
195	200	400	600	800	1000	1200

**Design of base pad:**

In EOS M270 machine, the minimum feature can be built only by using the support structure which is not possible by using direct part. In the case of a line support, laser only scans single pass thus the thickness of the line becomes one melt-pool thickness. Utilizing line support structure single bead deposits can be produced. Rectangular pads were built up from the base plate as the substrate for the single bead. The outer edge of the pad was supported by a solid support of height 4 mm and thickness 1.5 mm. The thickness of the pad is 3 mm on top of the support. Fig. 2 (a) and (b) shows different isometric views of rectangular pad.

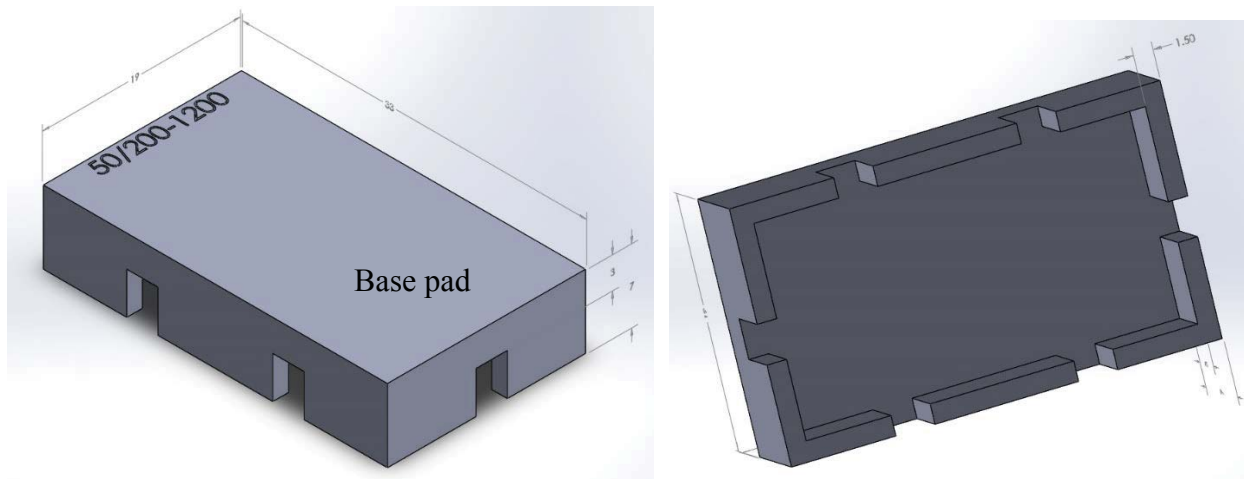


Fig. 2. (a) Top surface of the pad with a solid support (b) Bottom surface of the pad showing solid support of thickness 1.5 mm.

Rectangular thin walls of dimension 19 mm x 0.1mm x 0.06mm were made using Magics software and placed on top of the pad (Fig. 3). These are the sacrificial parts and only used to make single line support structure beneath the surface of these thin walls. Later these thin walls are deleted. Fig. 4 (a) shows a line support which was created under the thin wall. Fig. 4 (b) shows an array of line support. The overhanging surface of the pad was then filled with conventional block support (Fig. 5).

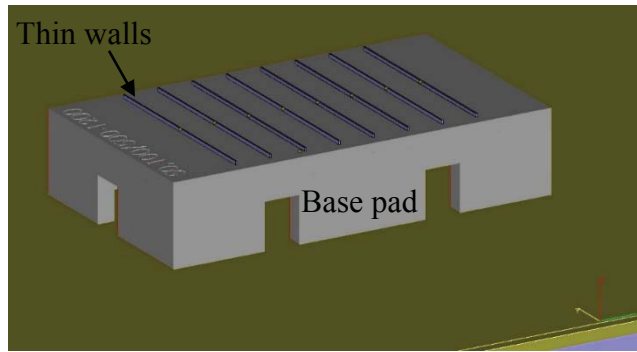


Fig. 3 Sacrificial thin walls were placed on top of the pad.

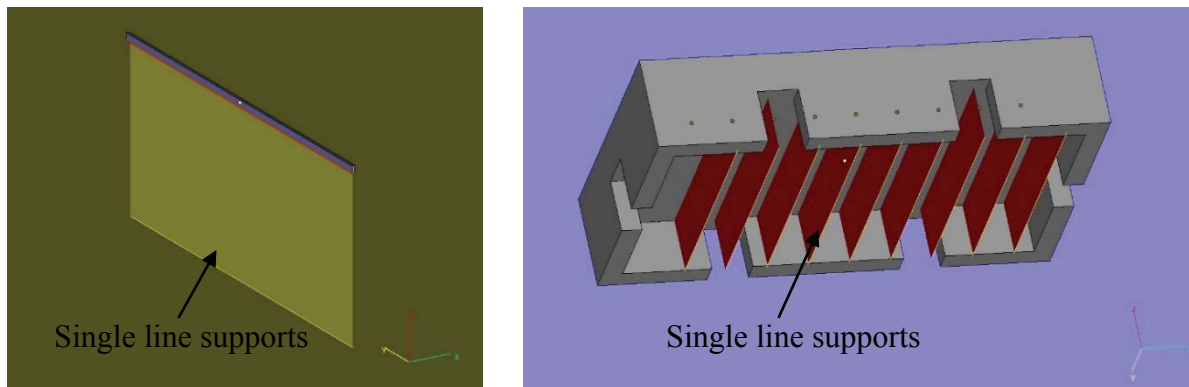


Fig. 4 (a) Building of a single line support beneath the sacrificial thin wall part. (b) An array of the single line supports running through the base pad.

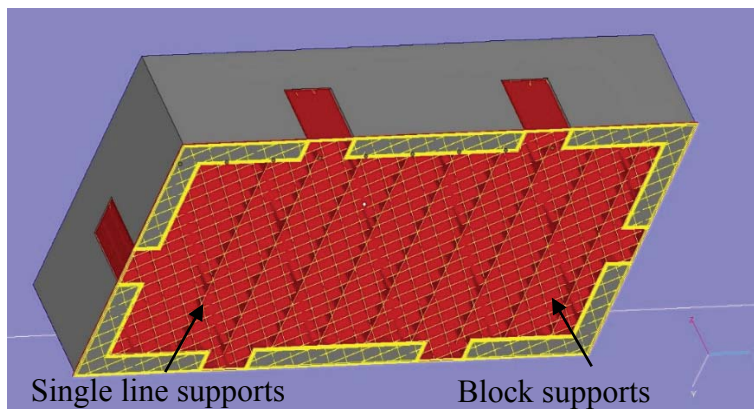


Fig. 5 Overhanging surface of the pad is supported by block support.

Once the line support has been created the thin walls on top of the pad, put to no exposure parameter so that the laser will not scan them. The parameters such as laser power and scan speed were applied to each of the line supports as listed in Table. 1. Upon laser scanning, the line support produces a thin wall of a width of one melt pool. The machine uses a scan strategy while processing the support structure parts in that it scans the support structure in every other alternate layer. A schematic presented in the Fig. 6 illustrates an alternate -layer-scan strategy used for

support structure construction. Every alternate layer, there will be a single track scanned for each line support with the assigned parameters. During the final layer scanning, soon after the base pad surface is scanned, single tracks scans will be exposed generating single bead deposits on the top of the base pad. Additional cube samples were also built using the various parameters. The single track deposits and bulk were examined under optical and SEM for morphology.

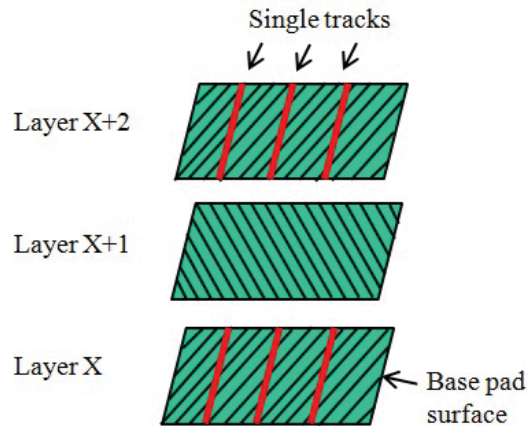


Fig. 6 Schematic illustrating the alternate layer support structure scan strategy

## Results and Discussion

Alloy IN 625 powder was characterized by SEM. Fig. 7a shows morphology and distribution of the powder particles. Particle size and distribution were determined by measuring the diameters of individual particles from several different SEM micrographs. It was estimated that particles have a particle size distribution between 15  $\mu\text{m}$  and 50  $\mu\text{m}$ . The powders showed spherical morphology. SEM shows the characteristic micro-dendritic structure of particles produced by atomization (Fig.7b). The larger particles were observed to have satellite particles attached. These small particles form due to fragment microdroplets sticking to the larger particles. The mean particle diameter was estimated around 40  $\mu\text{m}$ . The powders showed bimodal size distribution of the powder particles.

Differential scanning calorimetry curve for the alloy 625 during heating and cooling cycle is presented in Fig. 8. During the heating cycle, two distinct endothermic peaks were observed. First endothermic has the peak temperature at 1340°C and other at a higher temperature around 1445°C. The first peak represents melting temperature of the alloy IN625 [7], whereas the second peak is close to the melting of purer Ni. The presence of two peaks indicate that there was some segregation inside the particles, i.e.; purer regions of the core of the dendrites melt at 1445°C. During cooling one could observe the only solidification peak around 1297°C. DSC results explain that complete melting of the powder occurs about 1445°C, which is 100°C higher than the melting temperature of the alloy 1340°C. And solidification of was observed at 1297°C due to higher cooling in the DSC machine; it causes the alloy to be undercooled. Therefore, on can



expect in SLM of the alloy, the alloy during solidification can experience even higher undercooling as the cooling rates are very high during the process.

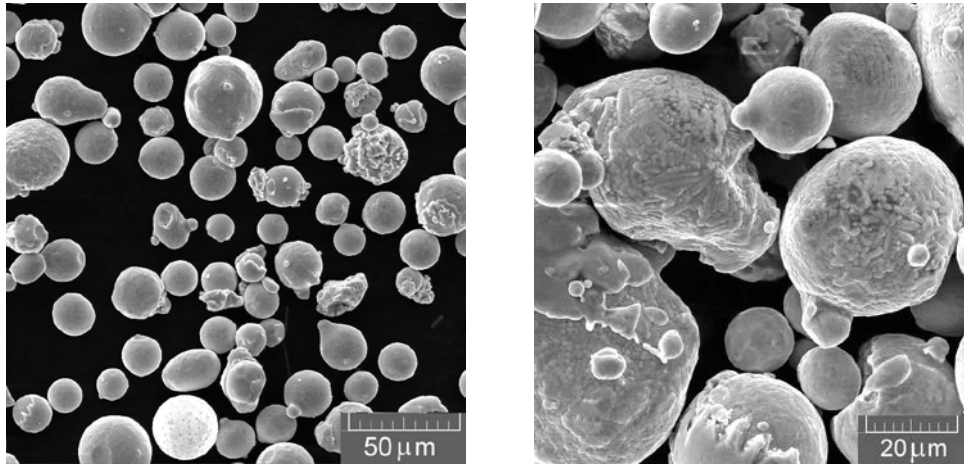


Fig.7 (a) Low magnification SEM micrograph of alloy IN625 powder (b) High magnification SEM micrograph of an individual powder particle.

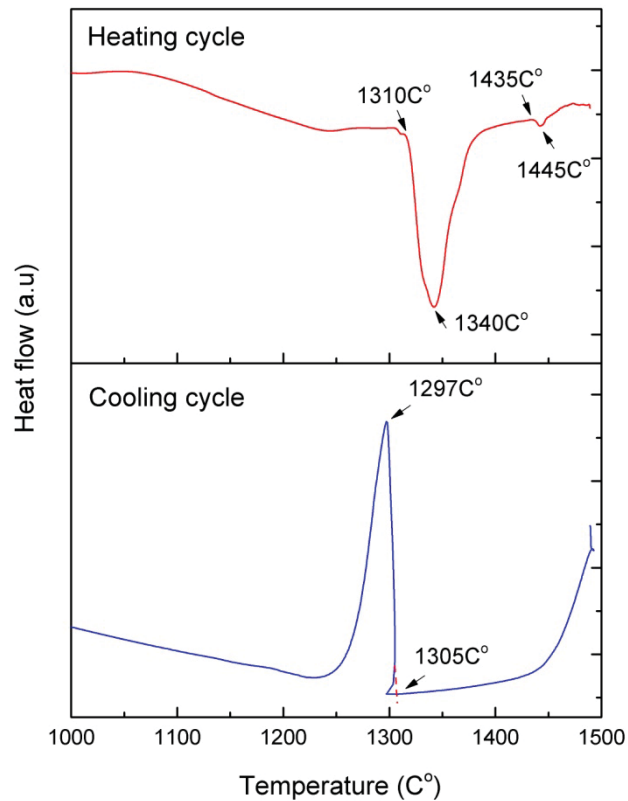


Fig. 8 DSC curves for alloy IN625 powder during heating and cooling.

Single track deposits were successfully made on the base pads using support structure scan strategy with various process parameters. Fig. 9 shows the photograph of the single track deposits and base pad. Each single track appears as a thin line on the base pad (indicated by an arrow).

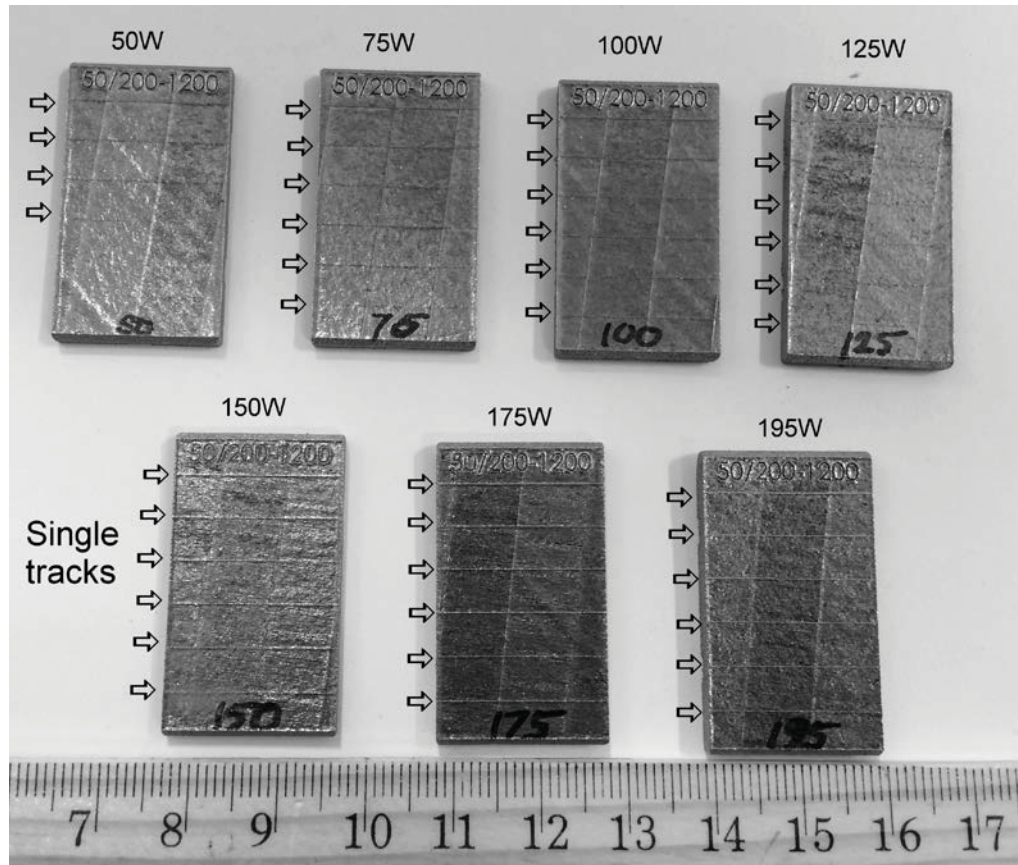


Fig. 9 Photograph of the single track deposits made on pad substrate. Arrows indicate single track deposits.

The top surfaces of the single line deposits were characterized by a SEM and the results are presented in Table 2. For the scan parameters with 50W and 200 mm/s, the single track deposit was observed to have a continuous and uniform deposit. As the scan speed was increased, the deposit becomes discontinuous, and eventually results in significant amount of balling, especially at 600 mm/s and 800 mm/s. The single track deposits with Laser power 50W with scan speeds of 1000 mm/s and 1200 mm/s did not show any trace of melting on the surface of the base pad. The absence of melt track was evidence that the laser power was insufficient to melt the powder since the laser scans at a faster rate, hence lower energy input. Also for higher scan speeds the melt track was irregular instead of straight track. The parameter combinations of high laser power and low scan speed (200mm/s), the incident high energy causes significant melting of powder resulting in a larger volume of melt pool size and wider spread of the bead deposit. In the case of higher laser scan speeds (eg.100W and 600mm/s, 800 mm/s, 125W, and 800 mm/s, 1000 mm/s), the bead surface was observed to have irregular, more rounded shape

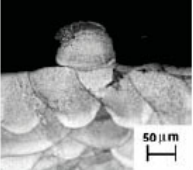

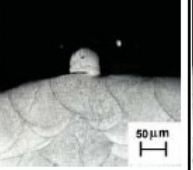
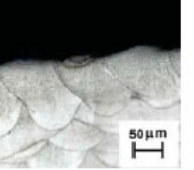
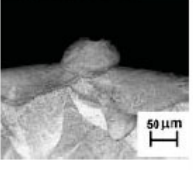
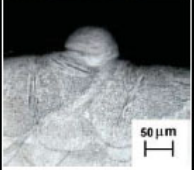
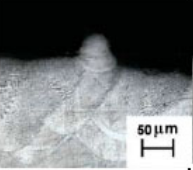
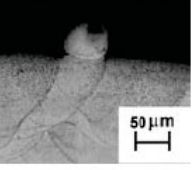
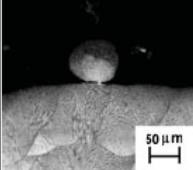
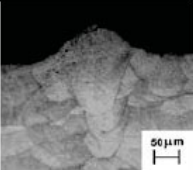
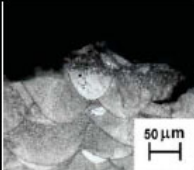
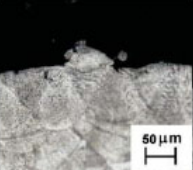
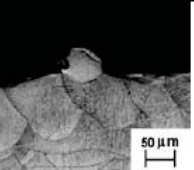
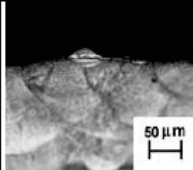
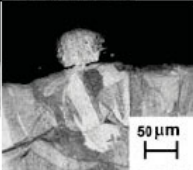
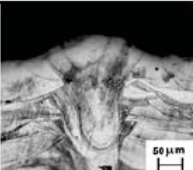
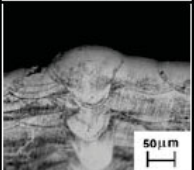
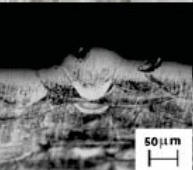
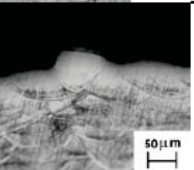
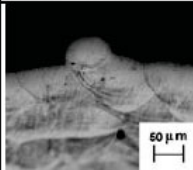
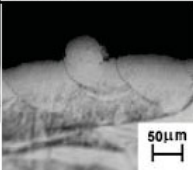
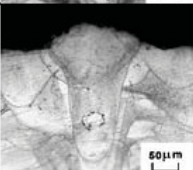
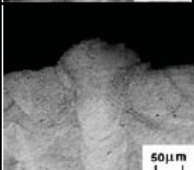
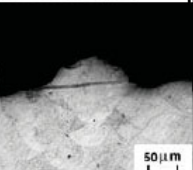
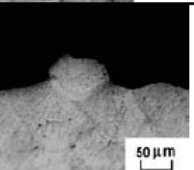
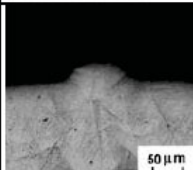
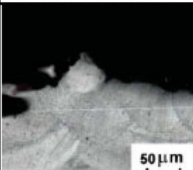
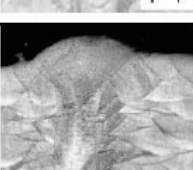
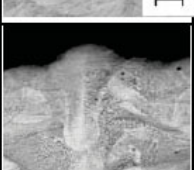

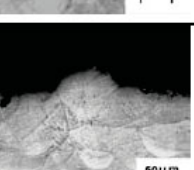
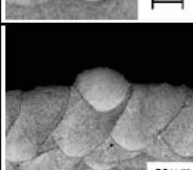
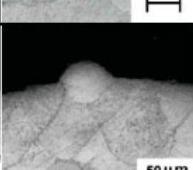

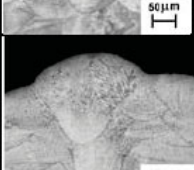
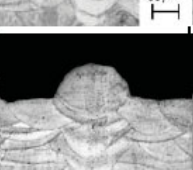
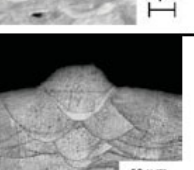
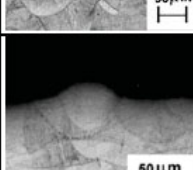
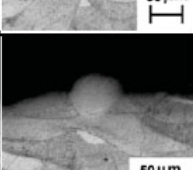
and bulging upwards, indicating that the surface tension forces of the melt region were dominant due less melt volume as dwell time of the laser was brief [8].

Table. 2 SEM micrographs of the top surface of the single track deposits

Laser Power	200 mm/s	400 mm/s	600 mm/s	800 mm/s	1000 mm/s	1200 mm/s
50W					No deposit / no melting	No deposit / no melting
75W						
100W						
125W						
150W						
175W						
195W						



Table. 3 Cross-section optical micrographs of the single track samples produced using various parameters

Laser power	200 mm/s	400 mm/s	600 mm/s	800 mm/s	1000 mm/s	1200 mm/s
50W					No track / no melting	No track / no melting
75W					Missing track in the cut section observed	
100W						
125W						
150W						
175W						
195W						

The single track deposits were sectioned and prepared for metallographic observations. The polished surfaces were etched with Kalling's reagent (CuCl<sub>2</sub> 5 gm., Ethanol 100 ml, HCl 100 ml). The etched cross-sections were presented in Table 2. The deposit morphology i.e., width and depth of the single track deposits can be clearly observed from the optical micrographs. At a power level 50W or 75W, with the slowest speed at 200 mm/s could melt a small region in the

base pad, and balling was prevalent in the deposit as the scan speed was increased. As the scan speed was increased, the energy density will be reduced; therefore lesser volume in the base pad was melted. Similar effects were observed for 100W and 125 W as well. The melt pool depth was observed to increase significantly for higher power (100 to 195W) and lower speeds. Similar to laser welding situation, in SLM at higher power levels and slower speeds conduction mode of welding/ deposition occurs resulting in deeper melt pools [9]. Keyhole shape of the melt pool was noticed to appear from the power levels 125W to 195 W for 200 mm/s scan speed. The deposits with power level 125W and above showed porosity in the lower regions of the melt pool. The formation of porosity in the single track deposits is attributed to the fall of the keyhole formed as soon as the laser beam passes. Once the laser beam (heat source) moves farther, the molten metal in the upper part of the keyhole drips downward to fill the keyhole due to gravity. During this, some vapor gets entrapped in the lower region of the keyhole, and this vapor cannot escape fully out of the melt pool because the surface of the bead exposed to cool inert gas gets solidified. Therefore, this mechanism leaves the pores behind in the deposits [10]. Therefore, higher powers and lower speeds should be avoided for overcoming such defects. The bowl-shaped melt pool was observed for power levels 125W to 195 W for medium scan speeds. This shape can provide optimum depth of melt pools and with sufficient hatch, overlap can provide a process window for arriving at desired optimum set of process parameters. Single track deposit width's and depth was measured according to the Fig. 10. The effect of process parameters on the width of the single track deposits is presented in Table. 4 and the results were plotted in Fig.8. The EOS M270 machine provides a laser beam diameter of 100  $\mu\text{m}$ . The measured width in some cases show values lower than that of beam diameter is corresponding to the balling in the deposits.

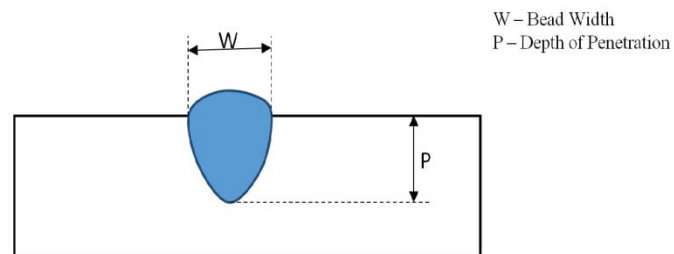


Fig. 7 Single Bead Geometry

Laser Power and scan speed have a significant effect on the single track bead width. The results indicate that, for constant power, an increase in speed leads to a decrease in width due to the laser beam traveling at high speed. Therefore the heat input decreases leading to less volume of the powder being melted per unit time; consequently, the width of the bead reduces. The results also show that laser power contributes an important effect in the bead width dimensions. An increase in laser power results in an increase in the width, because of the increase in the energy density. For low powers (e.g. 50, 75, 100 W), the resulting energy density is less that causes insufficient melting or balling. For higher power level (e.g. 125W and above for all speeds) consistent bead was found.

Table. 4 Single bead width's ( $\mu\text{m}$ ) for various power and speed levels. The reported values have a margin of error of  $\pm 3 \mu\text{m}$ .

		Laser Power (W)						
		195	175	150	125	100	75	50
Scan Speed (mm/s)	200	236	232	186	203	155	105	86
	400	206	162	154	140	105	86	Balling
	600	142	118	136	70	66	33	Balling
	800	128	118	97	103	67	Balling	Balling
	1000	100	104	99	94	50	Balling	Balling
	1200	92	90	66	80	Balling	Balling	Balling

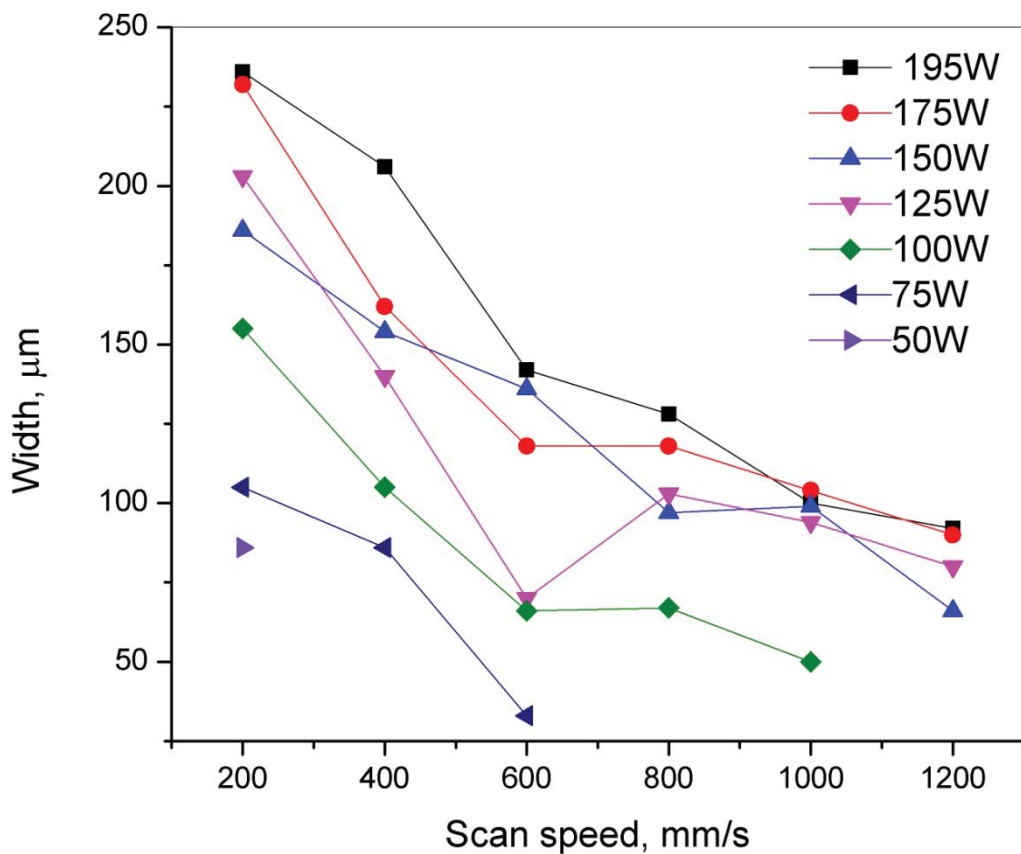


Fig. 8 Bead width for various processing parameters.

Table. 5 The depth of penetration ( $\mu\text{m}$ ) for various power and speed levels. The reported values have a margin of error of  $\pm 3 \mu\text{m}$ .

		Laser Power (W)						
		195	175	150	125	100	75	50
Scan Speed (mm/s)	200	272	265	220	204	127	25	10
	400	114	185	146	94	56	16	Balling
	600	46	110	73	69	12	14	Balling
	800	60	65	37	47	16	Balling	Balling
	1000	54	50	40	23	8	Balling	Balling
	1200	42	36	22	22	Balling	Balling	Balling

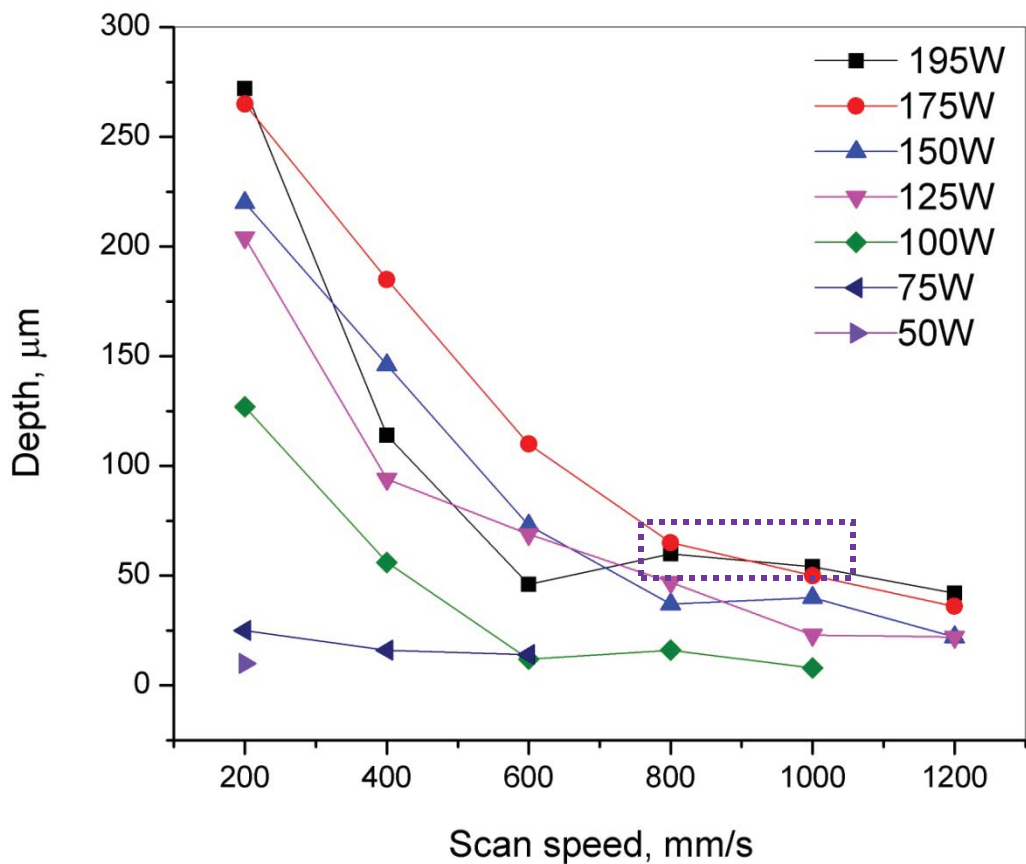


Fig.9 Depth of penetration for various processing parameters.



Table. 6 Depth to width ratios for various power and speed levels.

		Laser Power (W)						
		195	175	150	125	100	75	50
Scan Speed (mm/s)	200	1.15	1.14	1.18	1	0.82	0.24	0.12
	400	0.55	1.14	0.95	0.67	0.53	0.19	--
	600	0.32	0.93	0.54	0.99	0.18	0.42	--
	800	0.47	0.55	0.38	0.46	0.24	--	--
	1000	0.54	0.48	0.4	0.24	0.16	--	--
	1200	0.46	0.4	0.33	0.28	--	--	--

The depth of penetration of the single track deposits was measured and presented in Table 5. The effect of process parameters on the depth of penetration can be observed from Fig. 9. The results indicate that both laser power and scan speed are significantly affecting the penetration. When the energy density is high (high power - low speed), show deeper penetration occurs that can penetrate from 5 to 25 layers. Parameters indicated in the dotted box in Fig. 9 above have moderate energy density and provide consistent melt pool shape. Depth to width ratio on process parameters is presented in Table. 5. For the ratios with 0.4 to 0.6, the depth of penetration goes into 2-3 layer thickness that can ensure proper welding with the substrate with minimum porosity.

Further, bulk cube samples of dimensions 10 mm X 10 mm X 10 mm were fabricated using the parameters listed in Table.1. The cubes built using the parameters 75W and 200 mm/s, 100W and 200 mm/s, & 125W and 200 mm/s resulted in excessive balling / rounding with wavy nature of the surface. This rough surface led to jamming of the re-coater blade, and the build process was terminated for these samples. With the parameters mentioned above, a height of 1 mm was only possible to build before the re-coater was jammed. For the 125W, 200 mm/s the surface showed severe over melting and the sample did not build beyond 0.5 mm. Photograph of the cube samples built on a steel base plate is shown in Fig. 10. The samples were cut and prepared for microscopy studies. The as-polished cross-section surfaces of the as-built cubes are presented in Fig. 11. Energy density applied for building the cube samples is presented in Table 7. The effect or process parameters on the porosity/ density of the sample can be observed from the Fig. 11. For lower energy density samples, a significant amount of porosity was observed. The shape of the pores was noticed to have an irregular shape and sharper edges in the micrograph. As the energy density was increased, the porosity in the samples was observed to reduce. However, the higher energy density samples show rounded porosity which is a result of keyhole effect during the process [9]. Therefore, it is necessary to avoid the parameters result in melt pools which have keyhole shape and the also the parameters resulting in balling.

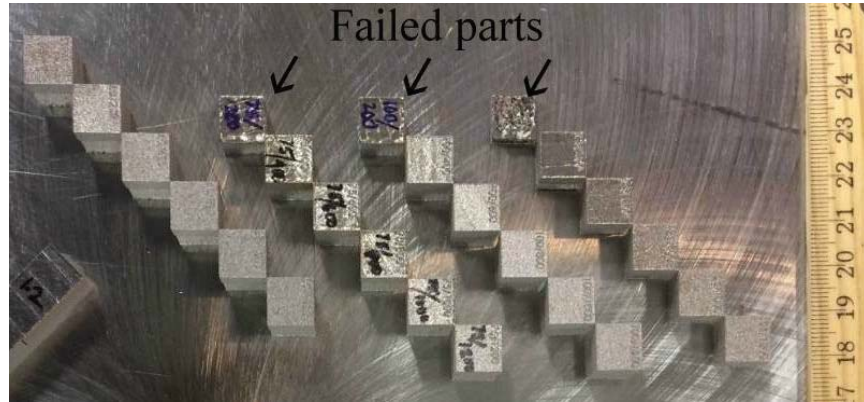


Fig. 10 Photograph of the cube samples build on a base plate. Note: Arrows indicate the parts whose build was terminated due to jamming of the re-coater blade.

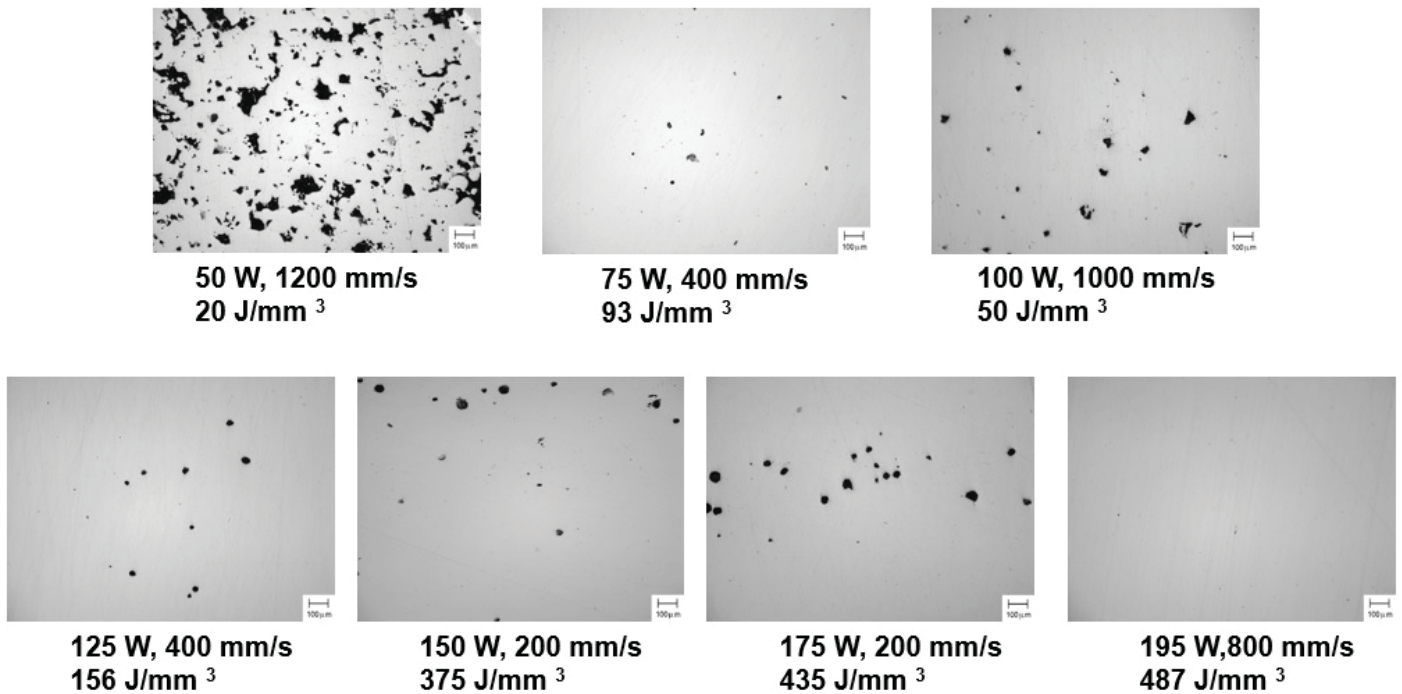


Fig. 11 As-polished optical micrographs of the cube samples showing variation in porosity with process parameters.

Table. 7 Energy density applied for building the cube samples with different process parameters

		Laser Power (W)						
		195	175	150	125	100	75	50
Scan Speed (mm/s)	200	487	435	375	312	250	187	125
	400	243	218	187	156	125	94	62
	600	162	145	125	104	83	62	41
	800	121	109	93	78	62	47	31
	1000	97	87	75	62	50	37	25
	1200	81	72	62	52	41	31	20

### Summary

The current work introduces a novel method of fabricating single track deposits using selective laser melting. The single track deposits were made using various scan parameters and their effect's on the width and depth of the deposit was studied. The study determines that as the scan speed increases, the width of the track decreases and become discontinues, eventually result in balling. The depth of penetration was observed to increase with the lower scan speed and higher power. Single track deposit's morphology can be utilized to select a narrow window of parameters for determining an optimum set of process parameters. The bulk deposits built with some parameters resulted in the failure of the builds due to jamming of the re-coater blade. The fully build samples showed a direct correlation to the energy density applied and the porosity evolution in the process. The process parameters with low energy density and high energy density both produced porosity, however, due to different reasons. An optimum laser power and scan speed can be recommended to produce near full-dense parts in the alloy 625.

### References

- [1] I. Gibson, D. Rosen, B. Stucker, Additive manufacturing technologies: rapid prototyping to direct digital manufacturing, Springer, New York, 2009.
- [2] Amit Bandyopadhyay, Susmita Bose, Additive Manufacturing, CRC Press, New York, 2015.
- [3] H. Miyanaji, S. Zhang, A. Lassell, A. A. Zandinejad, L. Yang, "Optimal process parameters for 3D printing of dental porcelain structures", in Proceedings of the Solid Freeform Fabrication Symposium, Austin, TX, USA, 2015.
- [4] J.J.S. Dilip and G.D. Janaki Ram, "Friction freeform fabrication of superalloy Inconel 718 – prospects and problems," Metallurgical and Materials Transaction *B*, Vol. 45, Issue 1, Feb. 2014, pp 182-192

- [5] Wen Shifeng, Li Shuai, Wei Qingsong, Chunze Yan, Zhang Sheng, Shi Yusheng, Effect of molten pool boundaries on the mechanical properties of selective laser melting parts, *Journal of Materials Processing Technology*, Volume 214, Issue 11, November 2014, Pages 2660-2667.
- [6] Haijun Gong, Hengfeng Gu, Kai Zeng, J.J.S. Dilip, Deepankar Pal, Brent Stucker, Melt Pool Characterization for Selective Laser Melting of Ti-6Al-4V Pre-alloyed Powder, *Solid Freeform Fabrication Symposium, Austin Texas 2014*, 256-267.
- [7] Stephen Floreen, Gerhard E. Fuchs, and Walter J. Yang, *The Metallurgy of Alloy 625*, TMS superalloys 1994, 13-37.
- [8] N. K. Tolochko, S. E. Mozzharov, I. A. Yadroitsev, T. Laoui, L. Froyen, V. I. Titov, M.B. Ignatiev (2004). Balling processes during selective laser treatment of powders. *Rapid Prototyping Journal*, 10, 78-87.
- [9] Antti Salminen, Josefine Svenungsson, Isabelle Choquet, Alexander F.H. Kaplan, 15th Nordic Laser Materials Processing Conference, Nolamp 15 Laser Welding Process – A Review of Keyhole Welding Modelling, *Physics Procedia*, Volume 78, 2015, Pages 182-191.
- [10] S. Pang, W. Chen, W. Wang (2014). A quantitative model of keyhole instability induced porosity in laser welding of titanium alloy. *Metallurgical and Materials Transactions A: Physical Metallurgy and Materials Science*, 45, 2808-2818.